POLYMORPHIC AND MORPHOLOGICAL MODIFICATIONS OF METAL CARBONATES

by

NICK NGUYEN

(Under the Direction of Tina T. Salguero)

ABSTRACT

In this thesis, the polymorphism and nanoscale synthesis of metal carbonates was explored. It is hypothesized that the stabilization of the metastable monoclinic phase in bulk group II metal carbonates occurs through the application of stabilizing anionic species such as sulfates and selenates. The monoclinic 10% $BaSO_4$ $BaCO_3$ was found to be stable when stored in anhydrous conditions while the monoclinic phase of 10% $SrSeO_4$ $SrCO_3$ was stable under atmospheric temperatures and humidity. These stabilizing anions were successfully introduced to the carbonate structure through a heat-quench reaction technique. The synthesis of metal carbonate nanoparticles was also explored using a methanol precipitation technique. In this work, the successful synthesis of non-group II metal carbonates such as $CdCO_3$ and $FeCO_3$ under ambient atmospheric and anhydrous conditions resulting in the precipitation of nanoparticles under 100 nm in lateral dimensions.

INDEX WORDS: Polymorphism; metal carbonate; stabilization; bulk; nano; methanol precipitation; precipitation; monoclinic; quench; quartz; ampoule; grind

POLYMORPHIC AND MORPHOLOGICAL MODIFICATIONS OF METAL CARBONATES

by

NICK NGUYEN

B.S., University of Georgia, 2015

A Thesis Submitted to the Graduate Faculty of The University of Georgia in Partial Fulfillment of the Requirements for the Degree

MASTER OF SCIENCE

ATHENS, GEORGIA

2018

POLYMORPHIC AND MORPHOLOGICAL MODIFICATIONS OF METAL CARBONATES

by

NICK NGUYEN

Major Professor:	Tina Salguero
Committee:	Paul Schroeder
	Jin Xie

Electronic Version Approved:

Suzanne Barbour
Dean of the Graduate School
The University of Georgia
August 2018

DEDICATION

To my loving parents, Thong and Kim Nguyen.

ACKNOWLEDGEMENTS

First, I would like to give thanks to my amazing parents, Thong and Kim Nguyen for all the love and support I have received from them as well as my closest and oldest friends the Davis family. I'd also like to thank all my close friends in the chemistry department who have made graduate school more than I expected in many ways.

I would like to thank my advisor, Professor Tina Salguero and my committee members Professor Paul Schroeder and Professor Jin Xie as well as Professor John Stickney for their dedicated guidance in my growth and development as a scientist and professional. Also to our collaborators in the Scott Beckman group at Washington State University including Professor Scott Beckman, Irmak Sargin and Bo Xu who were key to the development of my projects.

Finally, I would like to thank my group members from the Salguero lab both old and new for their companionship and mentorship. I have learned so much from every person I have met during my time in UGA's chemistry department. I offer a heartfelt thank you to you all for your role in my growth and education both personally and professionally.

TABLE OF CONTENTS

Page

CHAPTER 1

METAL CARBONATE INTRODUCTION AND LITERATURE REVIEW

Metal carbonates have been studied for centuries and as technology and science continue to progress, it has become apparent that there is still much to learn about them. With the development of nanoscience and the ability to characterize the structure and morphology of subjects on the nanoscale, metal carbonates have had a recent boon in a variety of research fields and applications. The study into the formation and stabilization of the various polymorphs of carbonate species is of interest to geological and biological sciences. Sea creatures such as clams and mollusks incorporate $CaCO_3$ and $MgCO_3$ into the production of shells and use them as templates for growth.

Metal carbonate mineral deposits are formed through a variety of natural conditions. They are also commonly formed through biogenic mechanisms such as the growth of shells by clams and mollusks as previously discussed as well as in hydrothermal deposits deeper in the crust where the temperature and pressure are higher. Recent results returning from the Mars rover observed carbonate species such as $MgCO_3$ on the surface of Mars[1].

Carbonates comprise a large proportion of the minerals found in the oceans and play a big role in the geochemistry of the worlds water cycle and the natural carbon sequestration process[2]. With the increased acidification of the oceans, these carbonaceous shells and sands are at risk of reacting and decaying through acid base neutralization reactions leading to their decomposition[3]. $CaCO_3$ alone is 4% of the earth's crust and can

be found as a major constituent of rock types such as limestone and chalk[4]. $BaCO_3$ and $SrCO_3$, although not as abundant as $CaCO_3$, are often found when barium and strontium substitute for calcium in the carbonate structure which occurs in up to 27% of $CaCO_3$ deposits[5].

Applications of Metal Carbonates

Metal carbonates can be used in the carbon capture and storage cycle where they serve as a storage medium for anthropogenic carbon emissions in a process which has been implemented in addition to the natural carbon sequestration cycles such as tree respiration to control the amount of free carbon species in the atmosphere[6].

They also are of interest to the fields of inorganic and materials science since metal carbonates are often used as precursor materials in applications where metal oxides are required such as the production of high purity alloys and compounds[7]. Metal carbonates decompose to form metal oxide species starting at 650° C under atmospheric conditions. In this form they find a wide field of applications ranging from metal alloy production[8] to coatings[9]. Strontium carbonate is used in the production of luminous paints[10] we well as in the production of drugs[11] and magnets[12].

The automotive industry relies on carbonates as a strengthener for plastics[13] and rubbers[14]. They have been applied in a variety of other roles ranging from cancer drug delivery[15] to the neutralization of dangerous sulfide species released during fracking[16]. $MgCO_3$ has a wide variety of applications ranging from fireproofing and fire extinguisher material to cosmetics and even can be found in toothpaste[17]. Due to their biocompatibility, metal carbonate species are often used in medical applications. Iron carbonate can be used

as an iron supplement to treat anemia, calcium carbonate is used as an antacid treatment and as a calcium supplement. Metal carbonates are also used as targeted treatment of certain illnesses such as manic-depressive disorder where Li_2CO_3 is commonly used as a mood stabilizer[18].

Beyond their applications as carbonates, metal carbonates will decompose to form reactive metal oxide species at elevated temperatures. Upon decomposition to their oxide species, they are particularly useful in the synthesis of high quality metal alloys and coatings. Metal carbonates are often used in the production of refractory ceramics and superconductive materials. Metal carbonates are commonly used as a precursor material for metal oxides that are highly reactive and cannot be stored as the oxide such as BaO or SrO. By using nano particles of carbonates, fresh metal oxides of greater reactivity can be made *in situ*, leading to more complete reactions and higher purity of products. This lends itself well to industrial applications like the production of high quality optics[19].

Nanoscale carbonates are currently of interest in other industrial and medical applications, for example, $BaCO_3$ has garnered interest to the field of cancer research[20] where it has proven to be an effective and biocompatible drug delivery vehicle. Nano carbonates are particularly desirable in medicine because of their biocompatibility and their high surface area which can be functionalized with gene attachments and other treatments. With higher surface area and larger surface area to volume ratio that is characteristic of nanoparticles, we can expect the reactivity of the material to be enhanced. In this thesis, the chemical and physical properties of metal carbonates will be examined as they are scaled down to the nano-regime and how they compare to the properties of their bulk counterparts.

Polymorphism of Metal Carbonates

At ambient conditions on the surface of the earth, the most energetically favored polymorphs of metal carbonates such as $SrCO_3$ or $BaCO_3$ are the trigonal and orthorhombic phases[21] (Figure 1). Other phases or polymorphs such as cubic, hexagonal and monoclinic phases exist as metastable phases resulting from high temperatures and pressures like those found in the earth's mantle and some are synthesized by organisms, such as coral and shell fish, which use a templating growth mechanism to achieve polymorph control.

In crystallography, alternate crystal structures which share an identical composition, such as the orthorhombic and cubic phases of metal carbonates, are known as polymorphs. For metal carbonates, polymorphs such as the cubic, monoclinic or hexagonal phases may exist as metastable or high temperature phases[22]. There are exceptions, some non-group II metal carbonates such as Li_2CO_3 may be found in the monoclinic phase in nature.[23] In nature, the polymorph of the carbonate structure is controlled through the pressure and temperature of the environment in most cases but there have also been reports of templated growth in marine animals [24].

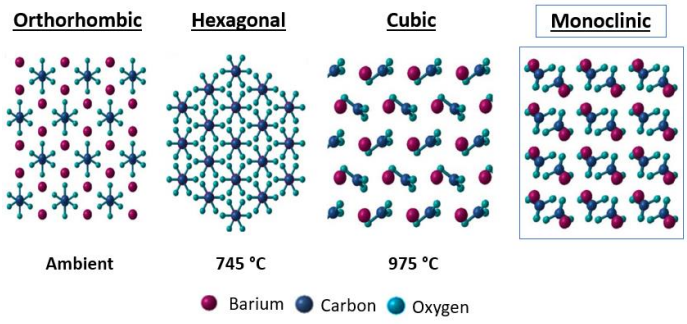

Figure 1: The most commonly found polymorphs for group II metal carbonates are the orthorhombic, hexagonal and cubic. The monoclinic phase has been reported as a high temperature/ pressure phase which is not stable at ambient conditions[21].

Traditional Syntheses of Metal Carbonates

Metal carbonates like calcium carbonate are mass produced by bubbling carbon dioxide gas through a suspension of calcium oxide in water. The bulk solid product is then removed from the solution and the dried, then is ground to the desired particulate size. This reaction provides little to no control over the particle size, surface roughness, or morphology of the resulting product, Flame spray pyrolysis, sonochemical, and solvothermal techniques are alternative techniques which allow some amount of control over the size and morphology of nano-scale carbonates although using organic capping agents or reactions which are highly wasteful and toxic. Templating schemes based on block co-polymers, upon which more complex structures of nano carbonates can be grown have also been examined as an approach that mimics the natural carbonate growth seen in nature. Here we will use an environmentally friendly synthetic method called the methanol precipitation technique which will be discussed later.

Research Goals

Control over the morphology and polymorphism of metal carbonates will be explored in two parts. The first will be the stabilization of bulk group II metal carbonates in the monoclinic phase through the incorporation of anions. In this work, the goal is to incorporate sulfate, selenate and phosphate anions into the structure of $BaCO_3$ and $SrCO_3$ using a heated quench synthesis technique. The second is the synthesis of metal carbonate nanoparticles using a non-traditional methanol precipitation approach. Here, the methanol precipitation technique was applied to synthesize metal carbonates such as $CdCO_3$, and $FeCO_3$.

References

1. Berner, R. A.; Morse, J. W., Dissolution kinetics of calcium carbonate in sea water; IV, Theory of calcite dissolution. *American Journal of Science* **1974,** *274* (2), 108-134.

2. Brown, A. J.; Hook, S. J.; Baldridge, A. M.; Crowley, J. K.; Bridges, N. T.; Thomson, B. J.; Marion, G. M.; de Souza Filho, C. R.; Bishop, J. L., Hydrothermal formation of clay-carbonate alteration assemblages in the Nili Fossae region of Mars. *Earth and Planetary Science Letters* **2010,** *297* (1-2), 174-182.

3. Figueroa, J. D.; Fout, T.; Plasynski, S.; McIlvried, H.; Srivastava, R. D., Advances in CO2 capture technology—the US Department of Energy's Carbon Sequestration Program. *International journal of greenhouse gas control* **2008,** *2* (1), 9-20.

4. Orr, J. C.; Fabry, V. J.; Aumont, O.; Bopp, L.; Doney, S. C.; Feely, R. A.; Gnanadesikan, A.; Gruber, N.; Ishida, A.; Joos, F., Anthropogenic ocean acidification over the twenty-first century and its impact on calcifying organisms. *Nature* **2005,** *437* (7059), 681.

5. Ono, S.; Kikegawa, T.; Ohishi, Y.; Tsuchiya, J., Post-aragonite phase transformation in CaCO3 at 40 GPa. *American Mineralogist* **2005,** *90* (4), 667-671.

6. Ayalon, A.; Bar-Matthews, M.; Kaufman, A., Petrography, strontium, barium and uranium concentrations, and strontium and uranium isotope ratios in speleothems as palaeoclimatic proxies: Soreq Cave, Israel. *The Holocene* **1999,** *9* (6), 715-722.

7. Lal, R., Carbon sequestration. *Philosophical Transactions of the Royal Society of London B: Biological Sciences* **2008,** *363* (1492), 815-830.

8. Jinrong, H., The Application and foreground of light calcium carbonate [J]. *Petrochemical Industry Application* **2009,** *2*, 004.

9. Carvalho, T. T.; Fernandes, J. R. A.; Perez de la Cruz, J.; Vidal, J. V.; Sobolev, N. A.; Figueiras, F.; Das, S.; Amaral, V. S.; Almeida, A.; Agostinho Moreira, J.; Tavares, P. B., Room temperature structure and multiferroic properties in Bi0.7La0.3FeO3 ceramics. *Journal of Alloys and Compounds* **2013,** *554* (0), 97-103.

10. Dimmick, A.; Mueller, K., High gloss calcium carbonate coating compositions and coated paper and paper board manufactured from same. Google Patents: 2006.

11. Georg, K., Luminescent material. Google Patents: 1955.

12. Chowdhury, E.; Maruyama, A.; Kano, A.; Nagaoka, M.; Kotaka, M.; Hirose, S.; Kunou, M.; Akaike, T., pH-sensing nano-crystals of carbonate apatite: effects on intracellular delivery and release of DNA for efficient expression into mammalian cells. *Gene* **2006,** *376* (1), 87-94.

13. Suresh, P.; Srinath, S., Observation of high coercivity in multiferroic lanthanum doped BiFeO3. *Journal of Alloys and Compounds* **2013,** *554* (0), 271-276.

14. Wei, W.; Ma, G.-H.; Hu, G.; Yu, D.; McLeish, T.; Su, Z.-G.; Shen, Z.-Y., Preparation of Hierarchical Hollow CaCO3 Particles and the Application as Anticancer Drug Carrier. *Journal of the American Chemical Society* **2008,** *130* (47), 15808-15810.

15. Momen, G.; Farzaneh, M., Survey of micro/nano filler use to improve silicone rubber for outdoor insulators. *Rev. Adv. Mater. Sci* **2011,** *27* (1), 1-13.

16. Zhao, Y.; Lu, Y.; Hu, Y.; Li, J.-P.; Dong, L.; Lin, L.-N.; Yu, S.-H., Synthesis of Superparamagnetic CaCO3 Mesocrystals for Multistage Delivery in Cancer Therapy. *Small* **2010,** *6* (21), 2436-2442.

17. Amosa, M.; Mohammed, I.; Yaro, S., Sulphide scavengers in oil and gas industry–a review. *Nafta* **2010,** *61* (2), 85-98.

18. Botha, A.; Strydom, C. A., Preparation of a magnesium hydroxy carbonate from magnesium hydroxide. *Hydrometallurgy* **2001,** *62* (3), 175-183.

19. Inoue, A.; Kong, F. L.; Han, Y.; Zhu, S. L.; Churyumov, A.; Shalaan, E.; Al-Marzouki, F., Development and application of Fe-based soft magnetic bulk metallic glassy inductors. *Journal of Alloys and Compounds* **2018,** *731*, 1303-1309.

20. Maurera, M.; Souza, A.; Soledade, L.; Pontes, F.; Longo, E.; Leite, E.; Varela, J. A., Microstructural and optical characterization of CaWO4 and SrWO4 thin films prepared by a chemical solution method. *Materials Letters* **2004,** *58* (5), 727-732.

21. Oganov, A. R.; Glass, C. W.; Ono, S., High-pressure phases of CaCO 3: crystal structure prediction and experiment. *Earth and Planetary Science Letters* **2006,** *241* (1), 95-103.

22. Shatskiy, A. F.; Litasov, K. D.; Palyanov, Y. N., Phase relations in carbonate systems at pressures and temperatures of lithospheric mantle: review of experimental data. *Russian Geology and Geophysics* **2015,** *56* (1–2), 113-142.

23. Milliman, J.; Müller, G.; Förstner, F., *Recent Sedimentary Carbonates: Part 1 Marine Carbonates*. Springer Science & Business Media: 2012.

24. Gutmann, B.; Chalup, A., Barium Carbonate. *American Ceramic Society Bulletin* **2000,** *79* (8), 63.

CHAPTER 2

ANION STABILIZATION OF MONOCLINIC METAL CARBONATES

Nguyen, Nick. To be submitted to CrystEngComm

Abstract

Sulfate and selenate anions will be incorporated into the carbonate structure through a heated quench synthesis technique. This approach was applied to study monoclinic strontium and barium carbonate[25] under ambient conditions (unsealed and reacted under atmospheric air), and inert conditions (sealed under a dry argon atmosphere) to explore the stability of their monoclinic polymorph. The stability of the monoclinic metal carbonate polymorph was explored under atmospheric conditions as well as under a humid environment and found to be sensitive to humidity. The incorporation of these anions to the structure make it possible to isolate a stable monoclinic polymorph as seen on Fourier transform infrared spectroscopy (FTIR) and powder X-ray diffraction (XRD) while having little to no impact on the polymorphic character of the carbonate species as seen through differential scanning calorimetry (DSC) and variable temperature X-ray diffraction (VT XRD).

Introduction to Anion Stabilized Metal Carbonates

The monoclinic carbonate structure is recognized as being a high temperature and pressure polymorph for group two metal carbonates. There is very little work on the isolation and study of metal carbonates in the monoclinic phase. One of the few reports of monoclinic carbonates is a study done with barium carbonate by Nishino[26] wherein barium sulfate was incorporated into the structure of barium carbonate. The resulting monoclinic barium carbonate polymorph was reported to be metastable, converting from monoclinic to the room temperature stable orthorhombic phase when exposed to water or upon heating to 700° C.

In addition to sulfates, alternative isostructural anions such selenates will be used as the anion incorporated to isolate the monoclinic phases of group II metal carbonates, this work will focus on strontium and barium carbonates[25]. The incorporation of anions is of interest to a variety of environmental and geochemical applications. In nature, carbonates are abundant and they will naturally experience dissolution and reprecipitation[22], during this process, there may be some degree of exposure to anions such as phosphates, selenates, and sulfates. This may lead to the formation of alternative carbonate polymorphs[27] which may be metastable.

The product of the ion incorporation may also result in the formation of what is known as a solid solution[28] where anions or cations may substitute into the structure of the carbonates. They may also occupy vacant sites, defect sites, or interstitial spaces within the structure. In a solid solution, although the ions are incorporated into the crystal structure of the carbonate, the product will still be observed as a single crystal phase.

The introduction of metal ions into the carbonate structure may occur in nature through another process known as sorption which occurs in two or three steps[29]. The first step is the adsorption of the ion to the surface of the mineral. Afterwards, the ion may continue to diffuse further into the bulk of the material where it may ultimately incorporate into the chemical structure forming a new polymorph or it may take a third step to precipitate out again, forming deposits on the interior or exterior of the mineral.

The metal cations selected for the incorporation may be a key factor in the stability of the polymorph as well. Larger cations such as the Sr^{2+} (1.95 Å)[30], and Ba^{2+} (2.15 Å)[30], which have been selected for this study, may have different coordination numbers in the structure than smaller cations such as Fe^{2+} (1.35 Å)[30] or Mg^{2+}(1.41 Å)[30]. Due to their larger ionic radii, we expect Sr and Ba cations will be more likely to successfully expand the unit cell dimensions of the carbonate structure to achieve the monoclinic polymorph.

For the purposes of this study, the goal will be to stabilize the monoclinic polymorph of barium and strontium carbonate using sulfates and selenates. The stability of the metal carbonate monoclinic phase will be studied, and the polymorphism of barium and strontium carbonate will be studied more thoroughly to examine the effects of anion incorporation into the crystal lattice.

Stabilization of Monoclinic Metal Carbonates with Sulfate Anions

Results and discussion

The synthesis of the monoclinic barium carbonates was done under atmospheric conditions. 10% $BaSO_4$ $BaCO_3$ was explored and it was found that using the heated quench synthesis method, the product was predominantly monoclinic under Fourier transform infrared spectroscopy (FTIR). The same synthesis was done with 10% $SrSO_4$ as well. In addition, parallel studies were done using $SrCO_3$ with 10% $BaSO_4$ and 10% $SrSO_4$. In all four studies, it was found that by adjusting the temperature of the heating (Table 1), it was possible to isolate a completely monoclinic product.

Table 1 The temperatures required to synthesize completely monoclinic products using the heat-quench technique.

Carbonate Species	Reaction temperature
10% $BaSO_4$ $BaCO_3$	870 °C
10% $SrSO_4$ $BaCO_3$	885 °C
10% $BaSO_4$ $SrCO_3$	885 °C
10% $SrSO_4$ $SrCO_3$	910 °C

The stability of the monoclinic polymorph was studied first under atmospheric conditions, then under an induced humid environment and it was found to be stable on the scale of hours when under atmospheric conditions with some monoclinic polymorph still present up to weeks later (Figure 2). When stored under humid conditions, it was found that the monoclinic phase began to diminish within minutes. Under humidity, the monoclinic carbonates converted back to their more energetically favored orthorhombic polymorph completely within hours of exposure.

The FTIR spectra of the group two metal carbonates has six characteristic peaks which identify the sample as being orthorhombic. 1436 cm^{-1}, 1070 cm^{-1}, 854 cm^{-1},

706 cm^{-1} and 689 cm^{-1}. Upon heating and quenching in the presence of the sulfate anions, we see that there is a distinct shift in some of these peaks. The peak shift which is of greatest importance is that of the peak at 854 cm^{-1}. This peak shift to 871 cm^{-1} indicates that the structure has been successfully converted to the monoclinic phase. In the spectra, the sulfate stretch is present in the 1350 cm^{-1}-1450 cm^{-1} range indicating that the sulfate anion's structure has been maintained after heating and quenching. Together, these vibrational modes from both the sulfate and the carbonate confirm that the monoclinic phase of the metal carbonate has been successfully isolated through the incorporation of the sulfate anion.

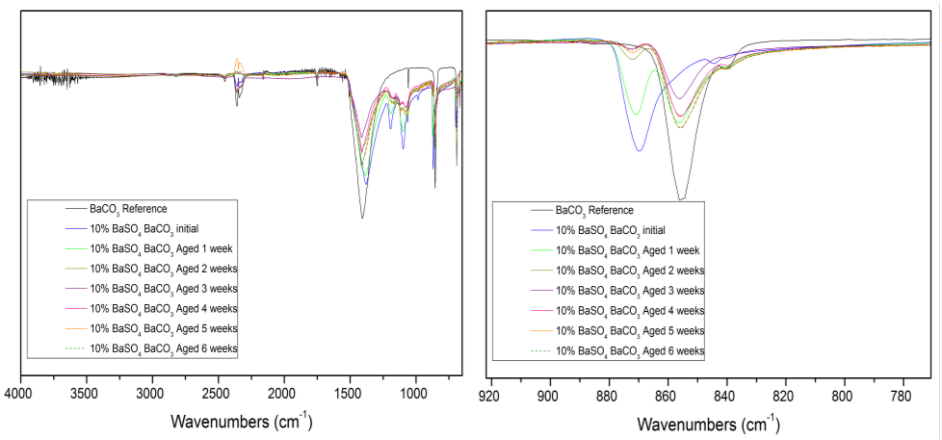

Figure 2: FTIR of 10% $BaSO_4$ $BaCO_3$ under ambient conditions, after 1 week the sample is mostly orthorhombic once more. Note the distinct peak shift from 854 cm^{-1} to 871 cm^{-1} which is indicative of the monoclinic phase.

When characterized by powder X-ray diffraction (XRD), the pattern for monoclinic $BaCO_3$ can be confirmed due to its characteristic peaks as confirmed through peak matching. The first is a set of characteristic peaks occur at 25 degrees (deg.) 2Θ, the second set is another set of three peaks which are centered at 31 deg. 2Θ under Co radiation. Together these two peak sets are the primary indicators of the monoclinic phase. The orthorhombic phase has an indicative peak set at around 28 deg. 2Θ under Co radiation.

Anhydrous synthesis of 10% $BaSO_4$ $BaCO_3$, 10% $SrSO_4$ BaCO3, 10% $BaSO_4$ SrCO3, and 10% $SrSO_4$ $SrCO_3$ were done to study the stability of their monoclinic polymorph. The synthesis procedure was found to be successful when the ampoules were sealed at pressures under 500 millitorr. It was found that when synthesized and stored anhydrously, the monoclinic polymorph of all four species were stable for extended periods of time, in the case of 10% $BaSO_4$ $BaCO_3$, the monoclinic polymorph was found to be the predominant phase for weeks after the synthesis. XRD of the sample in a sealed glass capillary showed that after 4 weeks there was only the beginnings of the conversion from the monoclinic phase to the orthorhombic phase at all as indicated in the slight growth of the peak set at 28 deg. 2Θ (Figure 3) under Co radiation.

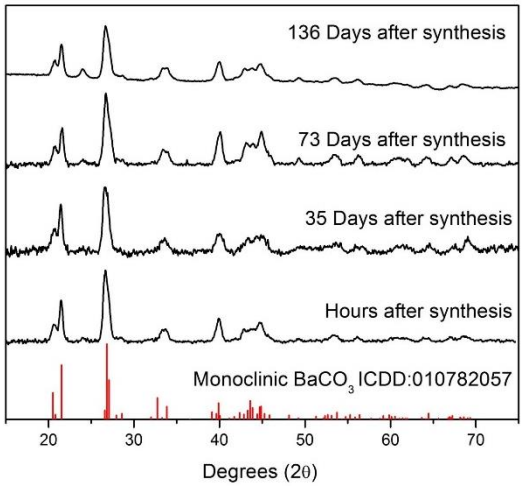

Figure 3: Powder XRD of 10% BaSO4 BaCO3 showing that even after more than 4 weeks the predominate phase is still the monoclinic polymorph.

Further studies into the polymorphism of the monoclinic barium and strontium carbonates was done via differential scanning calorimetry (DSC) and variable temperature X-ray diffraction (VT XRD). By cross referencing data gathered from DSC and VT XRD, it was possible to study the polymorphism of the anion stabilized carbonate species. For

thorough examination of the phase transitions of the samples, the temperature of the phase transitions was gathered from the DSC plots. From there, a separate sample of the same species was examined under VT XRD. Using VT XRD, it is possible to obtain crystallographic data of the sample at various temperatures while under inert atmosphere.

The monoclinic 10% $BaSO_4$ $BaCO_3$ species was first examined in DSC (Figure 4A). As the sample was heated in an argon atmosphere, the first prominent feature in the DSC plot (Figure 4A) is an exothermic peak with an onset temperature of 541° C which corresponds to an irreversible transition from the monoclinic phase to the orthorhombic phase. The second feature is an endothermic peak which has an onset temperature at 745° C corresponding to a transition from the orthorhombic phase to the trigonal/hexagonal phase of barium carbonate. The last distinct feature has an onset temperature at 944° C which corresponds to the transition from the hexagonal phase to the cubic phase.

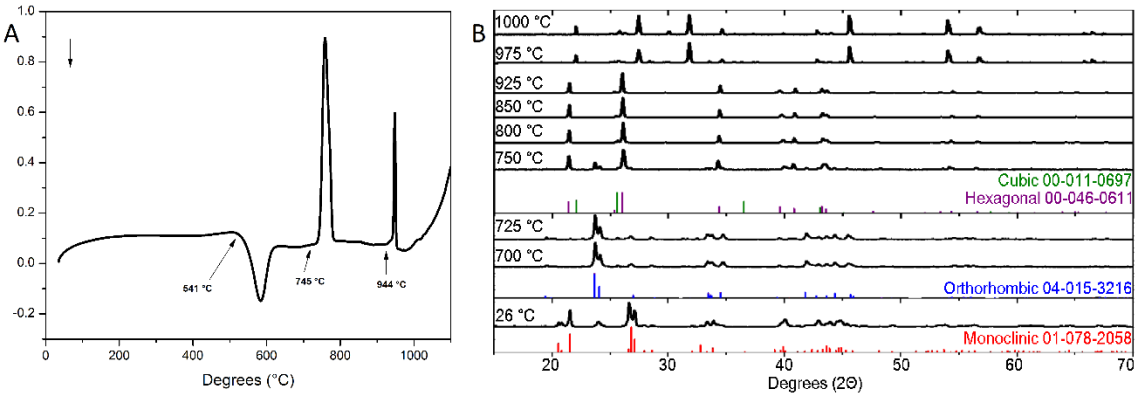

Figure 4: The DSC plot (A) and VT XRD patterns (B) for 10% $BaSO_4$ $BaCO_3$ note that the initial peak in (A) is an exothermic peak indicating that the conversion from monoclinic to orthorhombic is an irreversible reaction. Reference patterns in (B) are for the various polymorphs for $BaCO_3$ under Cu radiation.

Summary of Sulfate Reactions

For the sulfate stabilized monoclinic phase of both strontium and barium carbonate it has been proven that the monoclinic polymorph it is not an energetically metastable phase

as previously reported, but rather is a highly moisture sensitive phase which when kept anhydrous can be stored for extended periods of time. Further examination through DSC and VT XRD showed that the phase transitions for these carbonate species are not affected by the incorporation of the sulfate anions since the transition temperatures remain within 50° C of the transition temperatures previously reported for both carbonate species.[31]

Stabilization of Monoclinic Strontium Carbonate with Strontium Selenate

Results and discussion

The synthesis of the strontium selenate stabilized monoclinic barium carbonates was done under ambient atmospheric conditions. 10% $SrSeO_4$ $SrCO_3$ was explored and it was found that using the heated quench synthesis method, the product was predominantly monoclinic under XRD and FTIR. 10% $SrSeO_4$ $SrCO_3$ required heating to 1100° C to synthesize a completely monoclinic sample and the product presents as a white powder.

The stability of the monoclinic polymorph was studied first under atmospheric conditions, then under an induced humid environment and it was found to be exceptionally stable. When stored under ambient conditions, there is no sign that the monoclinic phase is converting to the orthorhombic phase even after one month. (Figure 5)

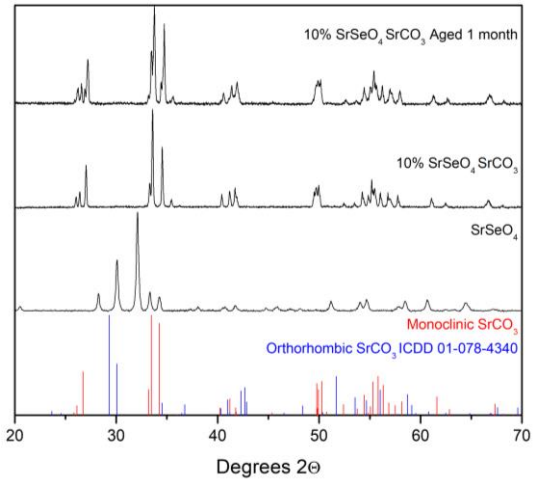

Figure 5: XRD pattern for 10% $SrSeO_4$ $SrCO_3$ shows that even when stored at ambient conditions for one month the sample has not converted to orthorhombic at all

The XRD of the product shows that there the selenate species has been completely incorporated. The pattern for the sample matches completely to the calculated pattern for monoclinic $SrCO_3$ as calculated by the Beckman group at Washington State University.

The monoclinic 10% $SrSeO_4$ $SrCO_3$ species has proven to be exceptionally stable even when exposed to humid environments as can be seen in the FTIR patterns in Figure 6.

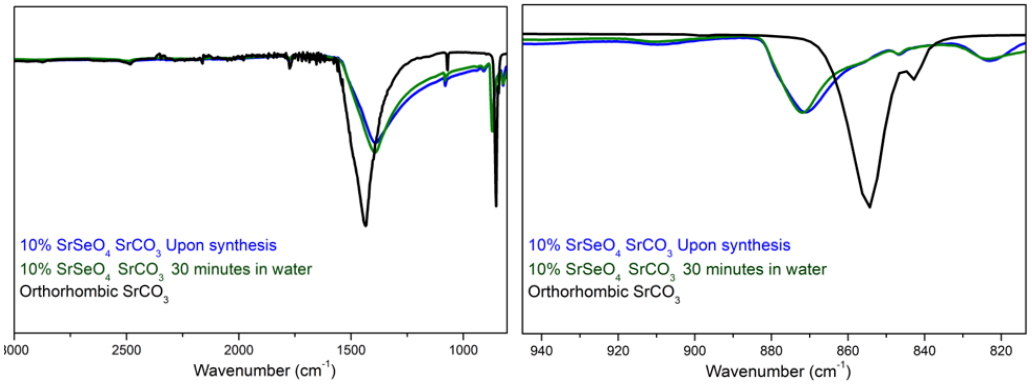

Figure 6: FTIR of 10% $SrSeO_4$ $SrCO_3$, the monoclinic phase has not been diminished even after the product was saturated in water and dried.

The monoclinic 10% $SrSeO_4$ $SrCO_3$ species was first examined in DSC (Figure 7). As the sample was heated in an argon atmosphere, the first prominent feature in the DSC plot is an exothermic peak with an onset temperature of 541° C which corresponds to an irreversible transition from the monoclinic phase to the orthorhombic phase. The second feature is an endothermic peak which has an onset temperature at 745° C corresponding to a transition from the orthorhombic phase to the trigonal/hexagonal phase of barium carbonate. The last distinct feature has an onset temperature at 944° C which corresponds to the transition from the hexagonal phase to the cubic phase.

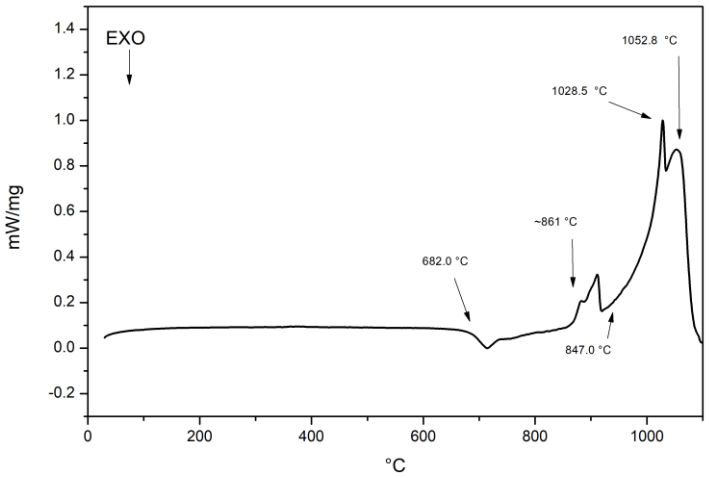

Figure 7: DSC of the monoclinic 10% $SrSeO_4$ $SrCO_3$ species. Note that the initial peak with an onset temperature of 682° C is an exothermic peak indicating that the conversion is non-reversible.

Experimental

Non-anhydrous Synthesis:

The reagents were hand ground in an agate mortar and pestle for 30 minutes then transferred into an open quartz ampoule. The ampoule was then placed into a pre-heated tube furnace and reacted for 30 minutes at which point it is carefully quenched into a salted ice bath making sure to prevent the submersion of the open end into the ice bath.

Anhydrous Synthesis:

The reagents were weighed out and hand ground in an Ar purged glovebox. The agate mortar and pestle should be heated in a drying oven for 30 minutes to drive off surface adsorbed water. The reagents were hand ground for 30 minutes in the glovebox. The sample was loaded into the ampoule which should then be sealed with a stopcock while under inert atmosphere. Upon removal from the glovebox, the ampoule was purged and refilled with pure argon on a schlenk line three times, then pumped down to 200 millitorr.

At this point the ampoule (still sealed by a glass stopcock) was submerged in liquid nitrogen bath for 15 minutes prior to having the glass ampoule sealed off. The 15 minutes in the liquid nitrogen are essential to allow for a successful sealing of the ampoule. If done without the cooling, the glass will fail as it softens due to the Ar gas expansion which is to be expected when the oxygen-acetylene torch is applied to seal off the ampoule. The ampoule was then loaded into a pre-heated tube furnace where it will react for 30 minutes before carefully quenching into a salted ice bath.

Materials and Methods:

$BaCO_3$ (≥99% purity), $SrCO_3$ (≥95% purity), and IR Grade KBr (≥99% trace metal basis) from Sigma Aldrich Corp. were used as received. $BaSO_4$ (reagent grade) and $SrSO_4$ (reagent grade) were used as received from J.T. Baker. $SrSeO_4$ was synthesized according to the synthetic procedure set forth by Errandonea [32] using $SrCl_2$ with $NaSeO_4$ purchased from Sigma Aldrich Corps. Quartz ampoules used for the reaction vessel were prepared in house by our glass shop. The furnace used in the reaction was the Lindburg/Blue M Mini-Mite tube furnace. 0.7 mm special glass capillaries from Charles supper were used to obtain anhydrous XRD of the samples.

For anhydrous preparation, the reagents were hand ground, then loaded into a schlenk vessel and capped with a teflon top. The vessel was then placed on a heating mantle set to 110° C and heated for 3 hours as a vacuum is pulled on it by a schlenk line to drive off humidity and produce an anhydrous reagent. The vessel was then closed tight upon completion of the dehydration step and placed into an Ar purged glovebox.

Non-anhydrous Characterization:

FTIR spectra were collected on a ThermoNicolet 6700 spectrophotometer using an ATR diamond and running OMNIC software package. XRD was done on a Bruker Advanced D8 diffractometer using Co Kα radiation.

Anhydrous Characterization:

XRD was done using a Bruker D8 Venture single crystal Diffractometer using Cu Kα radiation in sealed special glass capillary. KBR FTIR was done on a ThermoNicolet 6700 Spectrophotometer. DSC was done on a Netzsch STA 449 F3 Jupiter under argon atmosphere. VT XRD was done on a PANalytical XRD with an Anton-Parr 1200 heating furnace under argon atmosphere.

Computational work for the diffraction pattern and spectroscopy of monoclinic strontium carbonate was done by the Scott Beckman group at Washington State University by Bo Xu and Irmak Sargin under the supervision of Professor Scott Beckman.

Results and Conclusions

The incorporation of anions into the metal carbonate structure has made the isolation of their monoclinic polymorph possible at ambient conditions. Initial studies into the stabilizing effect of the sulfate anion revealed that the monoclinic barium carbonate structure was not merely an energetically or thermodynamically unfavorable phase, but rather one which was primarily susceptible to humidity. Upon isolating it from humidity,

the monoclinic barium carbonate could last on the scale of weeks with no sign of conversion to the orthorhombic phase

Strontium selenate was explored as a stabilizing anion for strontium carbonate. Strontium selenate is isostructural to strontium sulfate which made it an ideal candidate for this application. The monoclinic product of this reaction has proven to be less susceptible to conversion than in the sulfate studies. The monoclinic 10% $SrSeO_4$ $SrCO_3$ species was a shelf stable product even when stored non-anhydrously for longer periods of time than the sulfate stabilized products could withstand. Even when directly saturated with water, the monoclinic polymorph was still the predominant phase.

References

1. Brown, A. J.; Hook, S. J.; Baldridge, A. M.; Crowley, J. K.; Bridges, N. T.; Thomson, B. J.; Marion, G. M.; de Souza Filho, C. R.; Bishop, J. L., Hydrothermal formation of clay-carbonate alteration assemblages in the Nili Fossae region of Mars. *Earth and Planetary Science Letters* **2010,** *297* (1-2), 174-182.

2. Figueroa, J. D.; Fout, T.; Plasynski, S.; McIlvried, H.; Srivastava, R. D., Advances in CO2 capture technology—the US Department of Energy's Carbon Sequestration Program. *International journal of greenhouse gas control* **2008,** *2* (1), 9-20.

3. Orr, J. C.; Fabry, V. J.; Aumont, O.; Bopp, L.; Doney, S. C.; Feely, R. A.; Gnanadesikan, A.; Gruber, N.; Ishida, A.; Joos, F., Anthropogenic ocean acidification over the twenty-first century and its impact on calcifying organisms. *Nature* **2005,** *437* (7059), 681.

4. Ono, S.; Kikegawa, T.; Ohishi, Y.; Tsuchiya, J., Post-aragonite phase transformation in CaCO3 at 40 GPa. *American Mineralogist* **2005,** *90* (4), 667-671.

5. Ayalon, A.; Bar-Matthews, M.; Kaufman, A., Petrography, strontium, barium and uranium concentrations, and strontium and uranium isotope ratios in speleothems as palaeoclimatic proxies: Soreq Cave, Israel. *The Holocene* **1999,** *9* (6), 715-722.

6. Lal, R., Carbon sequestration. *Philosophical Transactions of the Royal Society of London B: Biological Sciences* **2008,** *363* (1492), 815-830.

7. Jinrong, H., The Application and foreground of light calcium carbonate [J]. *Petrochemical Industry Application* **2009,** *2*, 004.

8. Carvalho, T. T.; Fernandes, J. R. A.; Perez de la Cruz, J.; Vidal, J. V.; Sobolev, N. A.; Figueiras, F.; Das, S.; Amaral, V. S.; Almeida, A.; Agostinho Moreira, J.; Tavares, P. B., Room temperature structure and multiferroic properties in Bi0.7La0.3FeO3 ceramics. *Journal of Alloys and Compounds* **2013,** *554* (0), 97-103.

9. Dimmick, A.; Mueller, K., High gloss calcium carbonate coating compositions and coated paper and paper board manufactured from same. Google Patents: 2006.

10. Georg, K., Luminescent material. Google Patents: 1955.

11. Chowdhury, E.; Maruyama, A.; Kano, A.; Nagaoka, M.; Kotaka, M.; Hirose, S.; Kunou, M.; Akaike, T., pH-sensing nano-crystals of carbonate apatite: effects on intracellular delivery and release of DNA for efficient expression into mammalian cells. *Gene* **2006,** *376* (1), 87-94.

12. Suresh, P.; Srinath, S., Observation of high coercivity in multiferroic lanthanum doped BiFeO3. *Journal of Alloys and Compounds* **2013,** *554* (0), 271-276.

13. Wei, W.; Ma, G.-H.; Hu, G.; Yu, D.; McLeish, T.; Su, Z.-G.; Shen, Z.-Y., Preparation of Hierarchical Hollow CaCO3 Particles and the Application as Anticancer Drug Carrier. *Journal of the American Chemical Society* **2008,** *130* (47), 15808-15810.

14. Momen, G.; Farzaneh, M., Survey of micro/nano filler use to improve silicone rubber for outdoor insulators. *Rev. Adv. Mater. Sci* **2011,** *27* (1), 1-13.

15. Zhao, Y.; Lu, Y.; Hu, Y.; Li, J.-P.; Dong, L.; Lin, L.-N.; Yu, S.-H., Synthesis of Superparamagnetic CaCO3 Mesocrystals for Multistage Delivery in Cancer Therapy. *Small* **2010,** *6* (21), 2436-2442.

16. Amosa, M.; Mohammed, I.; Yaro, S., Sulphide scavengers in oil and gas industry–a review. *Nafta* **2010,** *61* (2), 85-98.

17. Botha, A.; Strydom, C. A., Preparation of a magnesium hydroxy carbonate from magnesium hydroxide. *Hydrometallurgy* **2001,** *62* (3), 175-183.

18. Inoue, A.; Kong, F. L.; Han, Y.; Zhu, S. L.; Churyumov, A.; Shalaan, E.; Al-Marzouki, F., Development and application of Fe-based soft magnetic bulk metallic glassy inductors. *Journal of Alloys and Compounds* **2018,** *731*, 1303-1309.

19. Maurera, M.; Souza, A.; Soledade, L.; Pontes, F.; Longo, E.; Leite, E.; Varela, J. A., Microstructural and optical characterization of CaWO4 and SrWO4 thin films prepared by a chemical solution method. *Materials Letters* **2004,** *58* (5), 727-732.

20. He, X. w.; Liu, T.; Chen, Y. x.; Cheng, D. j.; Li, X. r.; Xiao, Y.; Feng, Y. l., Calcium carbonate nanoparticle delivering vascular endothelial growth factor-C siRNA effectively inhibits lymphangiogenesis and growth of gastric cancer in vivo. *Cancer Gene Ther* **2008,** *15* (3), 193-202.

21. Oganov, A. R.; Glass, C. W.; Ono, S., High-pressure phases of CaCO 3: crystal structure prediction and experiment. *Earth and Planetary Science Letters* **2006,** *241* (1), 95-103.

22. Shatskiy, A. F.; Litasov, K. D.; Palyanov, Y. N., Phase relations in carbonate systems at pressures and temperatures of lithospheric mantle: review of experimental data. *Russian Geology and Geophysics* **2015,** *56* (1–2), 113-142.

23. Milliman, J.; Müller, G.; Förstner, F., *Recent Sedimentary Carbonates: Part 1 Marine Carbonates*. Springer Science & Business Media: 2012.

24. Gutmann, B.; Chalup, A., Barium Carbonate. *American Ceramic Society Bulletin* **2000,** *79* (8), 63.

25. Antao, S. M.; Hassan, I., The Orthorhombic Structure of $CaCO_3$, $SrCO_3$ $PbCO_3$ and $BaCO_3$: Linear Structural Trends. *The Canadian Mineralogist* **2009,** *47* (5), 1245-1255.

26. Nishino, T.; Sakurai, T.; Ishizawa, N.; Mizutani, N.; Kato, M., Characterization of a new SO2− 4-stabilized phase of BaCO3. *Journal of Solid State Chemistry* **1987,** *69* (1), 24-29.

27. Staudt, W. J.; Schoonen, M. A. A., Sulfate Incorporation into Sedimentary Carbonates. In *Geochemical Transformations of Sedimentary Sulfur*, American Chemical Society: 1995; Vol. 612, pp 332-345.

28. Chapter 3 Coprecipitation Reactions and Solid Solutions of Carbonate Minerals. In *Developments in Sedimentology*, Morse, J. W.; Mackenzie, F. T., Eds. Elsevier: 1990; Vol. 48, pp 87-132.

29. Sokolova, T. A.; Alekseeva, S. A., Adsorption of sulfate ions by soils (A Review). *Eurasian Soil Science* **2008,** *41* (2), 140-148.

30. Cordero, B.; Gómez, V.; Platero-Prats, A. E.; Revés, M.; Echeverría, J.; Cremades, E.; Barragán, F.; Alvarez, S., Covalent radii revisited. *Dalton Transactions* **2008,** (21), 2832-2838.

31. Ono, S.; Shirasaka, M.; Kikegawa, T.; Ohishi, Y., A new high-pressure phase of strontium carbonate. *Physics and Chemistry of Minerals* **2005,** *32* (1), 8-12.

32. Errandonea, D.; Muñoz, A.; Rodriguez-Hernandez, P.; Proctor, J. E.; Sapiña, F.; Bettinelli, M., Theoretical and experimental study of the crystal structures, lattice vibrations, and band structures of monazite-type PbCrO4, PbSeO4, SrCrO4, and SrSeO4. *Inorganic chemistry* **2015,** *54* (15), 7524-7535.

33. Chen, N.; Wan, C.; Zhang, Y.; Zhang, Y., Effect of nano-CaCO3 on mechanical properties of PVC and PVC/Blendex blend. *Polymer Testing* **2004,** *23* (2), 169-174.

34. Shaikh, S. F.; Mane, R. S.; Hwang, Y. J.; Joo, O.-S., Calcium carbonate electronic-insulating layers improve the charge collection efficiency of tin oxide photoelectrodes in dye-sensitized solar cells. *Electrochimica Acta* **2015,** *167*, 379-387.

35. Yin, L.; Cheng, H.; Mao, S.; Haasch, R.; Liu, Y.; Xie, X.; Hwang, S. W.; Jain, H.; Kang, S. K.; Su, Y., Dissolvable metals for transient electronics. *Advanced Functional Materials* **2014,** *24* (5), 645-658.

36. Kumar, M., Nano and microparticles as controlled drug delivery devices. *J. Pharm. Pharm. Sci* **2000,** *3* (2), 234-258.

37. Davidson, M. T., *Impact of nano-structuring on metal carbonates and metal titanates. [electronic resource]*. 2015.: 2015.

CHAPTER 3

SYNTHESIS OF METAL CARBONATE NANOPARTICLES AND CONCLUSIONS

Nguyen, Nick. To be submitted to CrystEngComm

Abstract

Nanoparticles of metal carbonates were successfully synthesized using an environmentally friendly, or “green”, synthetic methodology known as the methanol precipitation technique. The nanoparticles were found to range in size from 8-50 nm in diameter and have a uniform oblong morphology as confirmed by transmission electron microscopy (TEM). The crystal structure of the products was determined using powder X-ray diffraction (XRD) and selected area electron diffraction (SAED). Through tuning of the reaction conditions, the synthesis and characterized of non-group II metal carbonates were explored including $CdCO_3$ and $FeCO_3$.

Introduction to Methanol Precipitation Synthesis of Metal Carbonates

Nanoparticles of non-group II metal carbonates were explored using a methanol precipitation technique. In this application, nanoscale refers to particle sizes which are under 100 nm in lateral dimensions. Nanoscale metal carbonates are highly desirable due to their enhanced surface area and performance as additives in the synthetic rubber and plastics[33]. The electronics and power industries are interested in using nanoscale metal carbonates in applications such as insulating layers in solar cells[34] and as sources for high purity metal oxides for the production of field effect transistors[35].

Due to their scale, nanoparticles of metal carbonates have proven to have enhanced dispersing ability in addition to their high whiteness when used as a filler[33]. Since they have higher surface area compared to their bulk counterparts, they have attracted attention from the medical industry where researchers are looking to activate the surface of these particles to use them as drug delivery vehicles[36].

The methanol precipitation technique produces nanoparticles of metal carbonates on the scale of 10-200 nm in diameter[37]. The reaction proceeds through a dissolution-renucleation mechanism wherein the metal salt and sodium bicarbonate are dissolved in methanol and reacted at temperatures above the boiling point of methanol in a sealed vessel. As the precursors react to form the metal carbonate species, the product precipitates from the solution as the solubility of the carbonate species in methanol is lower than that of its precursors. The precipitation occurs rapidly as the reaction proceeds which result in the nanoscale morphologies which are of interest in this work.

This synthetic technique is highly desirable to industrial applications due to the low levels of waste produced. The only by-products of this synthetic technique are water,

sodium chloride and carbon dioxide gas. The precipitated product is pure since the other byproducts are either soluble in the solvent (NaCl), are a liquid (water) or will evolve from the solution as gas (CO_2). The methanol solvent can be reclaimed and purified indefinitely meaning that this is an exceptionally environmentally "green" reaction when compared to alternative syntheses to produce particles of comparable dimensions.

Initial research into the methanol precipitation technique showed that it was possible to synthesize nanoparticles of group II alkali earth metal carbonates. The size of the product could be varied in size from 40-200 nm by controlling the time and temperature of the reaction[37]. In this body of work, non-group II metal carbonates will be explored.

In this chapter, the synthesis of non-group II metal carbonates will be explored. The initial screening of carbonate species included both transition and main group metals which were stable in the 2+ charge state. The species which were explored can be found in Figure. Here, the synthesis and characterization of $CdCO_3$ and $FeCO_3$ will be discussed.

The synthesis of a wide variety of metal carbonate nanoparticles was explored using a methanol precipitation technique. Initial screening of metals which are stable in the 2+ covalent state showed that it was possible to synthesize more than just group II metal carbonates using this technique. It was found that in the successful reactions with non-group II metal chloride species required heating at a minimum of 90° C for at least 3 hours.

In some cases, the metal chloride species would be reduced to the metal species upon introduction to the methanol solvent. This is confirmed by the precipitation of the metal solid at the bottom of the schlenk vessel within a minute of the addition. This was found to be the case in the reactions with Pd, In, Ag and Tl chlorides.

It has been proven in the past that by using this technique, it is possible to synthesize the monoclinic polymorph of various group II metal carbonates. The reactions were also done anhydrously in an Ar purged glove box to preserve any possible metastable polymorph which may form because of the rapid formation and precipitation of the nanoparticles.

Synthesis and Characterization of $CdCO_3$ Nanoparticles

$CdCO_3$ was successfully synthesized using the methanol precipitation technique. The reaction for $CdCO_3$ took place over the span of 3 hours at 90° C. The product presents as a soft white powder upon completion of the reaction. Anhydrous reaction formed an identical product as confirmed by powder XRD and FTIR showing that there is no metastable polymorph being formed in this reaction.

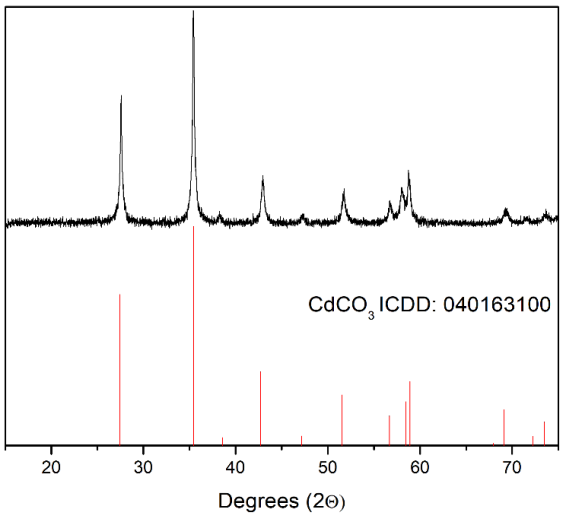

Figure 8: XRD of $CdCO_3$ as synthesized by the methanol precipitation technique

The diffraction pattern obtained from powder XRD (Figure 8) indicates that the product is pure $CdCO_3$, matching to the hexagonal phase of $CdCO_3$ (ICDD- 04-016-3100) which is the energetically preferred phase for this species. The peaks in the diffraction pattern of the sample show signs of peak broadening, a phenomenon which indicates that the product has very small grain boundaries or has very low dimensional morphology. Scherrer analysis of the peak widths in the diffraction pattern indicate that the average particle size in the sample is 49.7 nm.

TEM imaging of the product confirms that the product is a uniform distribution of nanoparticles. The product does aggregate when dried during the process of preparing the sample for imaging but measurements of the individual particles which make up the aggregate show that the particles range in size from 9 nm to 27 nm, with dimensions of most of the particles falling in the range of 9-15 nm in diameter.

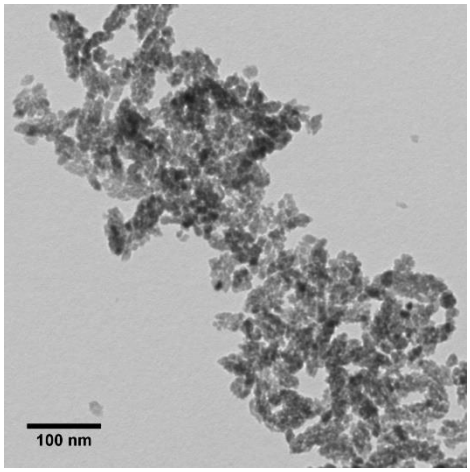

Figure 9: TEM imaging of $CdCO_3$ nanoparticles. The particles range in size from 9-27 nm with most of the particles falling in the range of 9-15 nm in lateral dimensions.

The variation between the Scherrer analysis of the particle size and the measurements could be due in part to the way the particles grow and precipitate. As the particles grow they may be growing in tandem, causing the orientation of their crystal structures, leading to larger coherent scattering domains which would be more represented in the XRD pattern which is indicative of the bulk product and may not represent the scattering domains of the smaller particles as strongly due to their smaller contributions to the diffraction pattern of the sample.

Varying the temperature from 90° C to 110° C and time from 3 hours to 24 hours of this reaction had no discernable effect on the particle size or morphology. This reaction could successfully produce $CdCO_3$ nanoparticles at an 60-70% yield which is to be expected using this synthetic approach. The product is stable in ambient conditions as confirmed by powder XRD and FTIR.

Synthesis and Characterization of $FeCO_3$ Nanoparticles

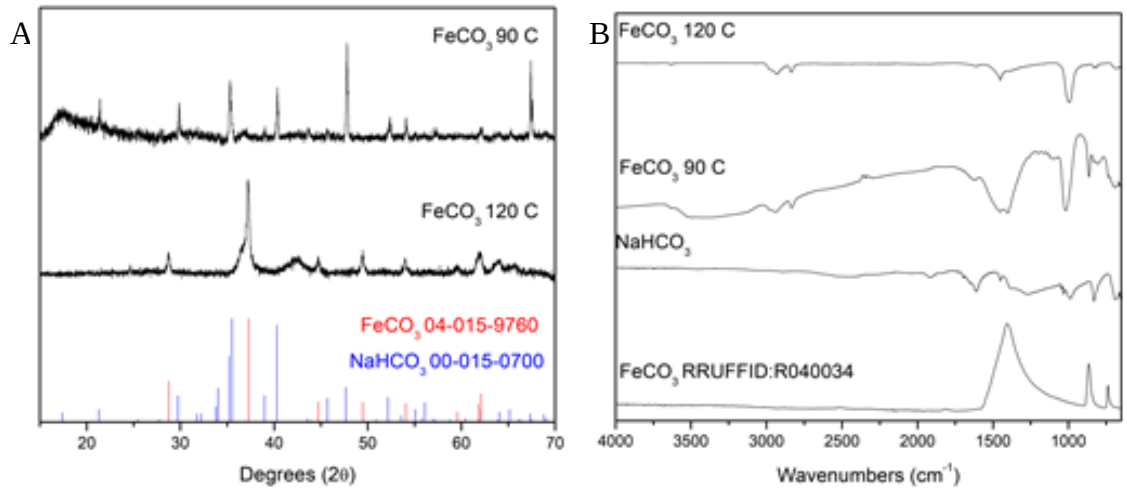

Figure 10: XRD(A) and FTIR (B) of $FeCO_3$ showing how adjusting the temperature of the reaction can help drive it to completion.

$FeCO_3$ was successfully synthesized both in ambient and anhydrous conditions. The product of the reaction is a pale green color which will begin to redden when exposed to ambient conditions as the product oxidizes to form iron oxide species. To preserve the initial product of the reaction, the reaction and characterization of $FeCO_3$ is done primarily anhydrously in an Ar purged glove box. The reaction was heated at 120° C for 3 hours.

Powder XRD of the sample as taken when loaded into a glass capillary and mounted on a powder diffraction stage show that by increasing the temperature of the reaction from 90° C to 120° C the reaction could go to completion (Figure 10). The peaks in this pattern match to the $FeCO_3$ reference number ICDD 04-015-9760.

KBr FTIR of the product shows a match to the $FeCO_3$ reference pattern as provided by the RRUFF database (RRUFF ID: R040034). The characteristic peaks at 870 cm^{-1} and at 748 cm^{-1} are present. There is a peak corresponding to $NaHCO_3$ at 1047 cm^{-1}. This indicates that there is some residual precursor material which has been retained in the sample.

Further characterization of the product was done using transmission electron microscopy (TEM) and selected area electron diffraction (SAED). The images of the $FeCO_3$ nanoparticles shows that the particles tend to aggregate much more than the $CdCO_3$ nanoparticles. Some aggregates were nearly a micron in lateral dimensions with some signs of the smaller particles still discernable in the images. The particles were nm in lateral dimensions on average. SAED of the aggregates prove that the sample is $FeCO_3$ matching to the D-spacings from $FeCO_3$ ICDD 04-015-9760.

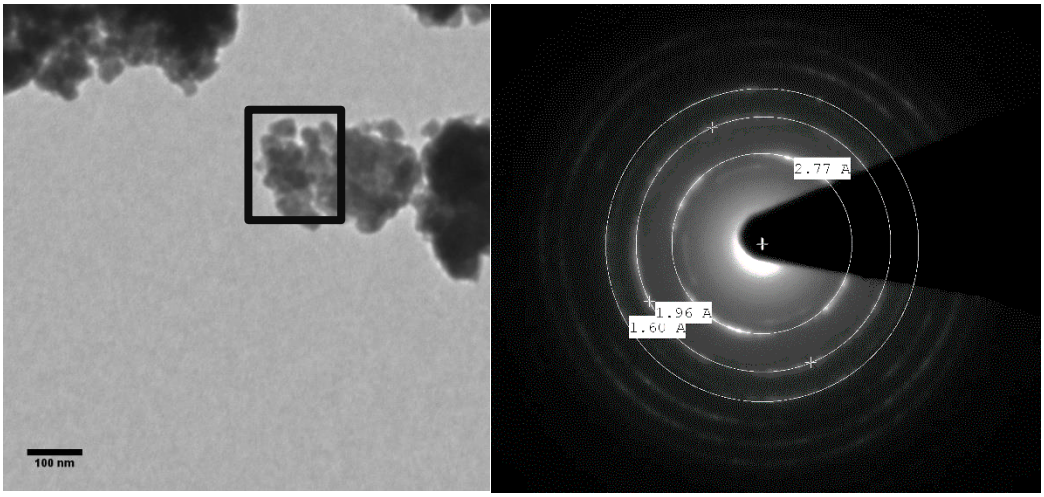

Figure 11: TEM image (left) and SAED (right) of the inset box area. FeCO3 particles agglomerate but the individual particles are still discernable. SAED matches to the D-spacings from ICDD reference pattern for FeCO3 04-015-9760.

Experimental

Non-anhydrous Synthesis:

The reagents for the reaction were the metal chloride species of the desired metal carbonate and $NaHCO_3$ in a 1.20:2.00 molar ratio and 20.0 mL of methanol. The reagents were added to a 100 mL schlenk vessel along with a stir bar and sealed using a teflon screw-on top. The schlenk vessel was suspended in a silicon oil bath which was be heated to 90° C and allowed to react for 3 hours. The time and temperature of the reaction may be

changed, and previous work has proven that these variables may affect the product morphology and success of the reaction. After the reaction has completed, the sample was cooled to room temperature before opening then the product is removed from the methanol via centrifugation and decanting of the solvent. The methanol used in the reaction may be saved, purified through roto-vap, and reused for these reactions indefinitely.

Anhydrous synthesis:

The reagents were prepared in a 1.20:2.00 molar ratio of anhydrous metal chloride to anhydrous $NaHCO_3$ reacted in 20.0 mL of anhydrous methanol. The stir bar and schlenk vessel was dried overnight in an oven or flamed to drive off adsorbed water prior to bringing into the glove box. The reaction was prepared in the glovebox, sealed then taken out to be suspended in a silicon oil bath at a temperature of at least 90° C for at least 3 hours. The sample was washed, and suction filtered in the glovebox and all preparations for characterization took place under argon atmosphere.

Materials:

$CdCl_2$ (technical grade), $FeCl_2 \cdot 4H_2O$ (≥99.0% purity), $FeCl_2$ (99.99% trace metal basis) and methanol (99.8% purity) were purchased from Sigma-Aldrich Corp. and used as received. $NaHCO_3$ (≥99.0% purity) from J.T. Baker was ground to a fine powder before use. IR Grade KBr (≥99% trace metal basis) from Sigma Aldrich Corp was used for KBr FTIR.

Non-anhydrous Characterization:

FTIR spectra were collected on a ThermoNicolet 6700 spectrophotometer using an ATR diamond and running OMNIC software package. XRD was done on a Bruker Advanced D8 diffractometer using Co Kα radiation.

Anhydrous Characterization:

Powder XRD was done using and on a Bruker D8 Bruker D8 Venture single crystal Diffractometer using Cu Kα radiation in sealed special glass capillary by Dr, Colin McMillen of Clemson Universities Molecular Structure Center. KBr FTIR was done on a ThermoNicolet 6700 Spectrophotometer. TEM/SAED was done with a Technai 20 electron microscope at 200 keV.

Table 2: Initial screening of metal species which are stable in the 2+ configuration yielded mixed results. The metal chloride species which showed some amount of carbonate production or reaction at all are included in the table here.

Metal Chloride Species			
Cd	Cu	Mg	Ni
Mn	Zn	Sn	Ru
Fe	La	Co	Rh

Discussion and Conclusions

Initial screening of metal species in the 2+ charge configuration saw mixed results. The reactions with the most promising products can be found on Table 2. The most successful reactions were the synthesis of $CdCO_3$ and $FeCO_3$. In the synthesis of these products it has become clear that the methanol precipitation technique is a powerful method of synthesizing uniform, pure nanoparticles of metal carbonates from other blocks of the periodic table. The product of the $CdCO_3$ synthesis matched to the diffraction patterns from both X-ray and electron diffraction and presented as uniform oblong particles under TEM.

The product was stable and was synthesized in the hexagonal phase which is the most energetically favored polymorph for $CdCO_3$ at ambient conditions.

It was also apparent that although the technique is capable of synthesizing metal carbonate species, the product is not always stable in ambient conditions. This was clear in the case of $FeCO_3$ where the diffraction pattern of the product matched to the reference $FeCO_3$ pattern when characterized under inert conditions but rapidly decomposed to form iron oxide species when stored under ambient conditions.

In conclusion, the monoclinic phase of $BaCO_3$ and $SrCO_3$ were successfully isolated through the incorporation of anions such as sulfates and selenates. The monoclinic phase proved to be stable at ambient conditions when strontium selenate was used as the stabilizing anion in $SrCO_3$ even upon saturation in water. Sulfate stabilized monoclinic $BaCO_3$ and $SrCO_3$ were proven to be highly sensitive to exposure to humidity, converting to the orthorhombic phase over the span of hours.

Non-group II metal carbonates were successfully synthesized using the methanol precipitation technique including $CdCO_3$ and $FeCO_3$ proving the versatility of the methanol precipitation method. The products were under 50 nm in lateral dimensions when characterized under XRD and TEM/SAED. The experimental parameters for the synthesis of further metal carbonate nanoparticles must be optimized for the reactions to go to completion.

References

1. Brown, A. J.; Hook, S. J.; Baldridge, A. M.; Crowley, J. K.; Bridges, N. T.; Thomson, B. J.; Marion, G. M.; de Souza Filho, C. R.; Bishop, J. L., Hydrothermal formation of clay-carbonate alteration assemblages in the Nili Fossae region of Mars. *Earth and Planetary Science Letters* **2010,** *297* (1-2), 174-182.

2. Figueroa, J. D.; Fout, T.; Plasynski, S.; McIlvried, H.; Srivastava, R. D., Advances in CO2 capture technology—the US Department of Energy's Carbon Sequestration Program. *International journal of greenhouse gas control* **2008,** *2* (1), 9-20.

3. Orr, J. C.; Fabry, V. J.; Aumont, O.; Bopp, L.; Doney, S. C.; Feely, R. A.; Gnanadesikan, A.; Gruber, N.; Ishida, A.; Joos, F., Anthropogenic ocean acidification over the twenty-first century and its impact on calcifying organisms. *Nature* **2005,** *437* (7059), 681.

4. Ono, S.; Kikegawa, T.; Ohishi, Y.; Tsuchiya, J., Post-aragonite phase transformation in CaCO3 at 40 GPa. *American Mineralogist* **2005,** *90* (4), 667-671.

5. Ayalon, A.; Bar-Matthews, M.; Kaufman, A., Petrography, strontium, barium and uranium concentrations, and strontium and uranium isotope ratios in speleothems as palaeoclimatic proxies: Soreq Cave, Israel. *The Holocene* **1999,** *9* (6), 715-722.

6. Lal, R., Carbon sequestration. *Philosophical Transactions of the Royal Society of London B: Biological Sciences* **2008,** *363* (1492), 815-830.

7. Jinrong, H., The Application and foreground of light calcium carbonate [J]. *Petrochemical Industry Application* **2009,** *2*, 004.

8. Carvalho, T. T.; Fernandes, J. R. A.; Perez de la Cruz, J.; Vidal, J. V.; Sobolev, N. A.; Figueiras, F.; Das, S.; Amaral, V. S.; Almeida, A.; Agostinho Moreira, J.; Tavares, P. B., Room temperature structure and multiferroic properties in Bi0.7La0.3FeO3 ceramics. *Journal of Alloys and Compounds* **2013,** *554* (0), 97-103.

9. Dimmick, A.; Mueller, K., High gloss calcium carbonate coating compositions and coated paper and paper board manufactured from same. Google Patents: 2006.

10. Georg, K., Luminescent material. Google Patents: 1955.

11. Chowdhury, E.; Maruyama, A.; Kano, A.; Nagaoka, M.; Kotaka, M.; Hirose, S.; Kunou, M.; Akaike, T., pH-sensing nano-crystals of carbonate apatite: effects on intracellular delivery and release of DNA for efficient expression into mammalian cells. *Gene* **2006,** *376* (1), 87-94.

12. Suresh, P.; Srinath, S., Observation of high coercivity in multiferroic lanthanum doped BiFeO3. *Journal of Alloys and Compounds* **2013,** *554* (0), 271-276.

13. Wei, W.; Ma, G.-H.; Hu, G.; Yu, D.; McLeish, T.; Su, Z.-G.; Shen, Z.-Y., Preparation of Hierarchical Hollow CaCO3 Particles and the Application as Anticancer Drug Carrier. *Journal of the American Chemical Society* **2008,** *130* (47), 15808-15810.

14. Momen, G.; Farzaneh, M., Survey of micro/nano filler use to improve silicone rubber for outdoor insulators. *Rev. Adv. Mater. Sci* **2011,** *27* (1), 1-13.

15. Zhao, Y.; Lu, Y.; Hu, Y.; Li, J.-P.; Dong, L.; Lin, L.-N.; Yu, S.-H., Synthesis of Superparamagnetic CaCO3 Mesocrystals for Multistage Delivery in Cancer Therapy. *Small* **2010,** *6* (21), 2436-2442.

16. Amosa, M.; Mohammed, I.; Yaro, S., Sulphide scavengers in oil and gas industry–a review. *Nafta* **2010,** *61* (2), 85-98.

17. Botha, A.; Strydom, C. A., Preparation of a magnesium hydroxy carbonate from magnesium hydroxide. *Hydrometallurgy* **2001,** *62* (3), 175-183.

18. Inoue, A.; Kong, F. L.; Han, Y.; Zhu, S. L.; Churyumov, A.; Shalaan, E.; Al-Marzouki, F., Development and application of Fe-based soft magnetic bulk metallic glassy inductors. *Journal of Alloys and Compounds* **2018,** *731*, 1303-1309.

19. Maurera, M.; Souza, A.; Soledade, L.; Pontes, F.; Longo, E.; Leite, E.; Varela, J. A., Microstructural and optical characterization of CaWO4 and SrWO4 thin films prepared by a chemical solution method. *Materials Letters* **2004,** *58* (5), 727-732.

20. He, X. w.; Liu, T.; Chen, Y. x.; Cheng, D. j.; Li, X. r.; Xiao, Y.; Feng, Y. l., Calcium carbonate nanoparticle delivering vascular endothelial growth factor-C siRNA effectively inhibits lymphangiogenesis and growth of gastric cancer in vivo. *Cancer Gene Ther* **2008,** *15* (3), 193-202.

21. Oganov, A. R.; Glass, C. W.; Ono, S., High-pressure phases of CaCO 3: crystal structure prediction and experiment. *Earth and Planetary Science Letters* **2006,** *241* (1), 95-103.

22. Shatskiy, A. F.; Litasov, K. D.; Palyanov, Y. N., Phase relations in carbonate systems at pressures and temperatures of lithospheric mantle: review of experimental data. *Russian Geology and Geophysics* **2015,** *56* (1–2), 113-142.

23. Milliman, J.; Müller, G.; Förstner, F., *Recent Sedimentary Carbonates: Part 1 Marine Carbonates*. Springer Science & Business Media: 2012.

24. Gutmann, B.; Chalup, A., Barium Carbonate. *American Ceramic Society Bulletin* **2000,** *79* (8), 63.

25. Antao, S. M.; Hassan, I., The Orthorhombic Structure of $CaCO_3$, $SrCO_3$ $PbCO_3$ and $BaCO_3$: Linear Structural Trends. *The Canadian Mineralogist* **2009,** *47* (5), 1245-1255.

26. Nishino, T.; Sakurai, T.; Ishizawa, N.; Mizutani, N.; Kato, M., Characterization of a new SO2− 4-stabilized phase of BaCO3. *Journal of Solid State Chemistry* **1987,** *69* (1), 24-29.

27. Staudt, W. J.; Schoonen, M. A. A., Sulfate Incorporation into Sedimentary Carbonates. In *Geochemical Transformations of Sedimentary Sulfur*, American Chemical Society: 1995; Vol. 612, pp 332-345.

28. Chapter 3 Coprecipitation Reactions and Solid Solutions of Carbonate Minerals. In *Developments in Sedimentology*, Morse, J. W.; Mackenzie, F. T., Eds. Elsevier: 1990; Vol. 48, pp 87-132.

29. Sokolova, T. A.; Alekseeva, S. A., Adsorption of sulfate ions by soils (A Review). *Eurasian Soil Science* **2008,** *41* (2), 140-148.

30. Cordero, B.; Gómez, V.; Platero-Prats, A. E.; Revés, M.; Echeverría, J.; Cremades, E.; Barragán, F.; Alvarez, S., Covalent radii revisited. *Dalton Transactions* **2008,** (21), 2832-2838.

31. Ono, S.; Shirasaka, M.; Kikegawa, T.; Ohishi, Y., A new high-pressure phase of strontium carbonate. *Physics and Chemistry of Minerals* **2005,** *32* (1), 8-12.

32. Errandonea, D.; Muñoz, A.; Rodriguez-Hernandez, P.; Proctor, J. E.; Sapiña, F.; Bettinelli, M., Theoretical and experimental study of the crystal structures, lattice vibrations, and band structures of monazite-type PbCrO4, PbSeO4, SrCrO4, and SrSeO4. *Inorganic chemistry* **2015,** *54* (15), 7524-7535.

33. Chen, N.; Wan, C.; Zhang, Y.; Zhang, Y., Effect of nano-CaCO3 on mechanical properties of PVC and PVC/Blendex blend. *Polymer Testing* **2004,** *23* (2), 169-174.

34. Shaikh, S. F.; Mane, R. S.; Hwang, Y. J.; Joo, O.-S., Calcium carbonate electronic-insulating layers improve the charge collection efficiency of tin oxide photoelectrodes in dye-sensitized solar cells. *Electrochimica Acta* **2015,** *167*, 379-387.

35. Yin, L.; Cheng, H.; Mao, S.; Haasch, R.; Liu, Y.; Xie, X.; Hwang, S. W.; Jain, H.; Kang, S. K.; Su, Y., Dissolvable metals for transient electronics. *Advanced Functional Materials* **2014,** *24* (5), 645-658.

36. Kumar, M., Nano and microparticles as controlled drug delivery devices. *J. Pharm. Pharm. Sci* **2000,** *3* (2), 234-258.

37. Davidson, M. T., *Impact of nano-structuring on metal carbonates and metal titanates. [electronic resource]*. 2015.: 2015.